Title
Diesel Exhaust Extract Exposure Induces Neuronal Toxicity by Disrupting Autophagy.

Journal
Toxicological sciences : an official journal of the Society of Toxicology, 176(1)

ISSN
1096-6080

Authors
Barnhill, Lisa M
Khuansuwan, Sataree
Juarez, Daniel
et al.

Publication Date
2020-07-01

DOI
10.1093/toxsci/kfaa055

Peer reviewed

OXFORD

SOT | Society of Toxicology
academic.oup.com/toxsci

TOXICOLOGICAL SCIENCES, 2020, 1–11

doi: 10.1093/toxsci/kfaa055
Advance Access Publication Date: April 16, 2020
Research article

Diesel Exhaust Extract Exposure Induces Neuronal Toxicity by Disrupting Autophagy

Lisa M. Barnhill,[*,†] Sataree Khuansuwan,[*,†] Daniel Juarez,[*] Hiromi Murata,[*,†] Jesus A. Araujo,[†,‡] and Jeff M. Bronstein[*,†,1]

[*]Department of Neurology; [†]Molecular Toxicology IDP; and [‡]Division of Cardiology, Department of Medicine, David Geffen School of Medicine, University of California Los Angeles, Los Angeles, California 90095

[1]To whom correspondence should be addressed at Department of Neurology, David Geffen School of Medicine, University of California Los Angeles, 710 Westwood Plaza, Los Angeles, CA 90095. Fax: 310 206-9819. E-mail: jbronste@mednet.ucla.edu.

ABSTRACT

The vast majority of neurodegenerative disease cannot be attributed to genetic causes alone and as a result, there is significant interest in identifying environmental modifiers of disease risk. Epidemiological studies have supported an association between long-term exposure to air pollutants and disease risk. Here, we investigate the mechanisms by which diesel exhaust, a major component of air pollution, induces neurotoxicity. Using a zebrafish model, we found that exposure to diesel exhaust particulate extract caused behavioral deficits and a significant decrease in neuron number. The neurotoxicity was due, at least in part, to reduced autophagic flux, which is a major pathway implicated in neurodegeneration. This neuron loss occurred alongside an increase in aggregation-prone neuronal protein. Additionally, the neurotoxicity induced by diesel exhaust particulate extract in zebrafish was mitigated by co-treatment with the autophagy-inducing drug nilotinib. This study links environmental exposure to altered proteostasis in an in vivo model system. These results shed light on why long-term exposure to traffic-related air pollution increases neurodegenerative disease risk and open up new avenues for exploring therapies to mitigate environmental exposures and promote neuroprotection.

Key words: air pollution; Alzheimer's disease; autophagy; diesel exhaust; dopaminergic neurons; neurodegeneration; Parkinson's disease; synuclein; ubiquitin proteasome system; zebrafish.

Air pollution is a well-accepted risk factor for respiratory and cardiovascular disease but only recently has it been implicated in neurodegenerative disorders. Several epidemiological studies have reported associations between exposure to air pollution and increased risk of Alzheimer's disease (AD), Parkinson's disease (PD), and cognitive decline (Dimakakou *et al.*, 2018; Fu *et al.*, 2019; Heusinkveld *et al.*, 2016; Hu *et al.*, 2019; Palacios, 2017; Ritz *et al.*, 2016; Shou *et al.*, 2019). Because more than 91% of the world is exposed to air quality below the WHO standards, the potential impact air pollution could have on disease prevalence is very large even if the effect size is relatively small. Much is known about exposure to air pollution increasing risk of asthma, cardiovascular disease, and stroke (Guarnieri and Balmes, 2014; Hoek *et al.*, 2001; Lee *et al.*, 2018; Mustafić *et al.*, 2012) but little is known about the mechanisms by which air pollution alters risk in neurodegenerative diseases.

The pathological hallmark of most neurodegenerative disorders is the accumulation of protein inclusions within and around neurons including amyloid beta in AD and alpha synuclein in PD (Ohama and Ikuta, 1976; Ross and Poirier, 2004; Spillantini *et al.*, 1997; Taylor *et al.*, 2002). In these diseases of aging, protein accumulation and neuronal loss lead to progressive neurological symptoms and cognitive decline over time. These disparate neurodegenerative diseases share common pathways associated with protein aggregation, suggesting an underlying commonality in disease etiology (Jellinger, 2010). Because genetic forms can only account for a small minority of disease incidence, it is quite likely that idiopathic forms of disease involve gene/environment interactions (Elbaz *et al.*, 2007; Goldman *et al.*,

2012; Lee *et al.*, 2015). Despite the fact that genetic forms of the diseases are rare, mutations and polymorphisms associated with these diseases have provided insight into important molecular pathways that confer susceptibility to neurodegeneration. Some of the proposed pathways include CNS inflammation, altered neuronal proteostasis, and mitochondrial dysfunction (Betarbet *et al.*, 2006; Ghiglieri *et al.*, 2018; Vegh *et al.*, 2019).

One of the major components of air pollution in urban environments comes from diesel exhaust. Intriguing data has come out of regions which experience heavy air pollution suggesting that exposure to diesel exhaust may contribute to protein aggregation and increase markers of neurodegeneration (Calderón-Garcidueñas *et al.*, 2008; 2012; Levesque *et al.*, 2011). In addition, animal models have shown neurotoxicity after exposure to air pollutants like diesel exhaust (Suzuki *et al.*, 2010; Yokota *et al.*, 2013). In order to determine the molecular pathways by which diesel exhaust might increase the risk of neurodegeneration, we utilized zebrafish (ZF) as a model organism and diesel exhaust particle extract (DEPe). DEPe is commonly used as a surrogate model of air pollution in health effects studies (Costa *et al.*, 2014; Hesterberg *et al.*, 2010; Levesque *et al.*, 2011). ZF are rapidly developing vertebrates with well-formed neuronal networks similar to that of mammals and are well suited for mechanistic studies of environmental toxins. The larvae are transparent so many pathological processes can be studied in intact living fish.

MATERIALS AND METHODS

Characterization of diesel exhaust particulate extract. A methanol extract of DEP (DEPe) was used for these studies and generated by sonication in methanol and resuspension in DMSO as described previously (Lawal *et al.*, 2015). The extract was submitted for further component analysis by Dr James Schauer from the University of Wisconsin-Madison. Total yield for each component was calculated in a spiked sample as well as the experimental sample and adjusted for dilution factor. The percent recovery of each compound was determined using a spiked sample and this was used to adjust the final concentration of each compound identified in the DEPe. The presence of 120 compounds was analyzed and final concentration calculated (Supplementary Table 1).

ZF treatment. ZF DEPe treatments were conducted on dechorionated embryos/larvae between 24 and 120 hours post fertilization (hpf) in 0.5× E2 embryo media (7.5 mM NaCl, 0.25 mM KCl, 0.5 mM $MgSO_4$, 0.075 mM KH_2PO_4, 0.025 mM Na_2HPO_4, 0.5 mM $CaCl_2$, and 0.35 mM $NaHCO_3$) with a final concentration of 0.1% DMSO vehicle. Typically, 20 embryos were treated per well in a final volume of 5–10 ml. ET*vmat2*: eGFP ZF which express eGFP in aminergic neurons under the vesicle monoamine transporter (*vmat2*) promoter (Wen *et al.*, 2008) as well as *isl*:GFP ZF which express eGFP in sensory neurons under the *islet1* promoter (Palanca *et al.*, 2013) were utilized for neurotoxocity assays. DEPe was added at 10–25 μg/ml and embryos were incubated for 24 h with treatment, except for morphology/mortality experiments, which were kept in treatment through the course of the experiment. In all other studies, DEPe was washed out 3× in E2 media and embryos were grown up to 72 or 120 hpf for fixation or in vivo analysis.

ZF behavior assay. ZF embryos that had been dechorionated were treated between 24 and 48 hpf with DEPe, washed out, and grown up to 7 days post fertilization (dpf). Behavior analysis was conducted on embryos that were morphologically normal as published previously using the ZebraBox, and data were collected using ViewPoint ZebraLab (ViewPoint Behavior Technology, Civrieux, France) software (Lulla *et al.*, 2016). Briefly, larvae were transferred into a square 96-well plate with 12 larvae per condition and were acclimated in the dark for 20 min before recording movement. Behavior was captured for 1 h with light cycling of 10 min light/10 min dark for 3 cycles. Data were analyzed by averaging the distance moved per larvae during each 10 min increment.

ZF neuron counts. After DEPe treatment, 3 or 5 dpf ET*vmat2*: eGFP ZF larvae were anesthetized in <0.01% tricaine-S (tricaine methanesulfonate Western Chemical, Ferndale, Washington) and fixed in 4% paraformaldehyde. Larvae were washed in PBS, antibody labeled, and cleared in 100% glycerol before mounting for confocal imaging at 20× magnification on a Leica SPE (Leica Microsystems Inc., Buffalo Grove, Illinois). For *islet1* neuron counts, embryos were live imaged. For *vmat2* neuron counts, fixed larvae were labeled as follows: larvae were permeablized with Proteinase K (03115828001, Sigma Aldrich, St Louis, Missouri) at 10 μg/ml, washed, and blocked in 5% BSA + 5% goat serum. Primary antibody incubation with monoclonal mouse-anti GFP antibody (A11120, ThermoFisher Scientific, Waltham, Massachusetts) followed by washes and secondary antibody incubation with goat-anti mouse AlexaFluor 488 (A11001, ThermoFisher Scientific).

For neuron counts, z-stacks containing 40–60 optical sections were collected for each ZF brain 1–2 μm apart. Aminergic neurons in the telencephalon, diencephalon, and raphae clusters were quantified using ImageJ in a blinded and randomized fashion. Peripheral sensory neurons were quantified by treating Tg(*isl1[ss]:Gal4-VP16,UAS:eGFP*) (Khuansuwan *et al.*, 2019) embryos and imaging at 10× magnification (Leica SPE) in the tail region of 5 dpf larvae. Neuron numbers were quantified in ImageJ in a blinded and randomized fashion. Neuron counts were normalized within each experiment to the vehicle-treated control group.

RT-PCR primers and assay. Quantitative RT-PCR was conducted in 96-well plates using a BioRad CFX Connect (Bio-Rad Laboratories, Hercules, California). All data were normalized to housekeeping control gene *elfa* (elongation factor 1B). Primers used as follows:

ZF *elfa* Forward Primer: 5′-CTTCTCAGGCTGACTGTGC-3′
ZF *elfa* Reverse Primer: 5′-CCGCTAGCATTACCCTCC-3′
ZF *sncg1* Forward Primer: 5′-ATGGTGGTATGGAAGGAGGA-3′
ZF *sncg1* Reverse Primer: 5′-GGGCTCAGGGAAAGTCTTTT-3′

Samples were run using the BioRad SsoAdvanced SYBR Green Supermix (172-5271 Bio-Rad Laboratories) under conditions recommended by the manufacturer. All data were calculated using double delta Ct relative to internal housekeeping gene expression.

Western blot. For analysis of ZF proteins, larvae were anesthetized in tricaine and decapitated on ice before protein was extracted from approximately 50 heads per condition in SDS sample buffer (63 mM Tris, 10% glycerol, and 3.5% SDS). Human cells were treated in 6-well plates for 24 h with 0.1% DMSO vehicle control, 10 μg/ml DEPe, or pepstatin A (P5318-5MG, Sigma Aldrich) at 10 μg/ml with E64D at 5 μg/ml (BML-PI107-0005, Enzo Life Sciences Farmingdale, New York) before direct lysis in RIPA with protease inhibitors (80–200 μl/sample). All samples were

sonicated briefly on ice before centrifugation. Protein concentration of the supernatant was established by BCA assay.

For each sample, 25–50 μg of protein was loaded and run on a 12% SDS-PAGE gel (ZF) or 12% Bolt bis-tris gel (human) with 1× loading dye and 2-mercaptoethanol in a final volume of 25 μl. Protein was transferred to nitrocellulose membrane using the XCell-II blotting system (ThermoFisher Scientific). Membrane was blocked in 5% nonfat milk and probed with antibodies as follows: polyclonal rabbit-α-Sncg1 1° antibody (1:1000) generated as described previously (Lulla *et al.*, 2016) followed by donkey-α-rabbit HRP 2° antibody (1:2500) (sc-2313, Santa Cruz Biotechnology, Dallas, Texas); monoclonal mouse-α-tubulin 1° antibody (1:10 000) (T9026, Sigma Aldrich) followed by goat-α-mouse HRP 2° antibody (1:10 000) (62-6520, ThermoFisher Scientific); rabbit α lc3B 1° antibody (1:1000) (NB100-2220, Novus Biologicals Centennial, Colorado) followed by biotinylated goat-α-rabbit 2° antibody (1:2500) (BA-1000, Vector Laboratories Burlingame, California) and streptavidin HRP diluted 1:250 (SA-5014, Vector Laboratories); mouse α tubulin 1° antibody (1:10 000) (T9026, Sigma Aldrich) followed by goat α mouse HRP 2° antibody (1:10 000) (62-6520, ThermoFisher Scientific). Blots were developed in chemiluminescent substrate ECL Plus (32132, ThermoFisher Scientific) and exposed to film for band visualization. Quantification of bands was done in ImageJ using the gel analysis feature. For Sncg1, the band corresponding to tetrameric protein was quantified (~55 kDa) and normalized to α-tubulin (~50 kDa). For lc3II/lc3I ratios, band intensity for both lc3I (~17 kDa) and lc3II (~15 kDa) was measured and displayed as a ratio.

FACS analysis of SK-GFPu. Human neuroblastoma SK-N-MC cells stably transfected with CMV: GFPu were grown as described previously (Wang *et al.*, 2006). Briefly, cells were grown at 37°C and 5% CO_2 in DMEM with 10% FBS and supplemented with penicillin/streptomycin. Cells were 60%–80% confluent and treated in 24-well plates with DMSO vehicle (0.5% DMSO), 2.5 μM of clasto-Lactacystin β-lactone (L7035, Sigma Aldrich), or DEPe between 10 and 25 μg/ml. All treatments were incubated at 37°C for 24 h before FACS analysis. After treatment, 1 μg/ml propidium iodide (P-3566, ThermoFisher Scientific) was added to wells for 30 min. Cells were released in trypsin and immediately sorted using a Beckman Coulter Epics XL-MCL flow cytometer.

ZF autophagy assay. For autophagy studies, transgenic ZF expressing eGFP-tagged lc3 under the neuronal promoter *elavl3*, Tg(*elavl3:eGFP:map1lc3b*) (Khuansuwan *et al.*, 2019) were utilized, known as *huc:eGFP:lc3* onwards (Khuansuwan *et al.*, 2019). Experiments were done as published previously. Briefly, ZF were treated between 48 and 72 hpf before in vivo imaging via confocal microscopy (Leica SPE) and analysis of autophagosome number.

Single larvae were anesthetized with <0.01% tricaine and mounted in 1% agarose into a 35/12 mm glass-bottom culture dish (64-0757, Warner Instruments, Holliston, Massachusetts). For quantification of punctae, z-stacks of eGFP-Map1lc3b-positive optic tectum regions were acquired using a 40× oil immersion objective (NA = 1.15) and a 488-nM excitation laser line. Each z-stack comprised 13 1024 × 1024 pixel sections with a z-step size of 2 μm. Three nonconsecutive sections from the optic tectum z-stack were quantified for punctae number.

Nilotinib rescue. Rescue experiments were conducted by co-treating *vmat2*: eGFP embryos with 25 μg/ml DEPe and the autophagy-inducing drug nilotinib (CDS023093, Sigma Aldrich) at a concentration of 10 μM. At 48 hpf, DEPe was washed out and embryos were retreated with nilotinib for the remainder of the experiment. Neurons were imaged by confocal microscopy and analyzed relative to vehicle controls in ImageJ as described previously (Lulla *et al.*, 2016).

Statistical methods. The following statistical methods were utilized: Behavioral analysis utilized a two-way ANOVA with repeated measures. Aminergic neuronal comparisons were analyzed using a one-way ANOVA with Sidak's multiple comparisons analysis. Sensory and serotonergic neuron loss was analyzed using an unpaired two-tailed Student's *t* test. Proteasome assay results were analyzed by a one-way ANOVA with Dunnett's multiple comparisons analysis and lysosomal inhibition in SK-N-MC cells and Sncg1 blots were analyzed using a paired Student's *t* test. Autophagic flux in ZF was analyzed using an unpaired Student's *t* test. One-way ANOVA with Dunnett's multiple comparison analysis was used to analyze the effects of nilotinib on neuron counts after DEPe exposure.

RESULTS

ZF represent a unique transitional in vivo model system for studying neurodegeneration and molecular pathways involved in neurotoxicity (Bandmann and Burton, 2010; Martin-Jimenez *et al.*, 2015). General toxicity of DEPe in developing ZF embryos was determined by exposing embryos to 1–25 μg/mL DEPe through 7 dpf. Significant cardiac edema and tail curvature were detected at 20 μg/ml (Figure 1A). Exposure of ZF to 20 μg/ml of DEPe through 7 dpf led to increased lethality and significant morphological abnormalities. Because the majority of treated ZF survived through 5 dpf at a concentration of 10–25 μg/ml, experiments were done within this range unless otherwise noted. Additionally, in all subsequent experiments, DEPe treatment was washed out after exposure between 24 and 48 hpf in order to avoid mortality and morphological impairment.

Although ZF behavioral phenotypes can be directly related to neurotoxicity or represent a more global toxicity, they can be useful as a screening tool, as has been shown in previous environmental exposures to pesticides like ziram (Lulla *et al.*, 2016). At 7 dpf, morphologically normal larvae show reproducible light cycling behavior, moving more under dark conditions relative to light conditions. DEPe treatment resulted in no change in movement under dark conditions, but total movement was significantly reduced in 2 of 3 light cycles relative to untreated controls (Figure 1B). This indicates DEPe-induced toxicity even when the toxin has been washed out and the larvae appear morphologically normal.

After establishing behavioral toxicity, it is important to determine if this correlates with a toxicity that may be relevant to neurodegeneration. ZF embryos from the transgenic line ET*vmat2*: eGFP, which expresses eGFP in aminergic neurons (dopaminergic, noradrenergic, and serotonergic) under the control of the vesicle monoamine transporter (*vmat2*) promoter, were treated between 24 and 48 hpf, washed out, and raised to 3 or 5 dpf before quantification of neuronal clusters (Figs. 2A and 2B). This brief exposure to DEPe led to progressive loss of eGFP-positive neurons in both the telencephalon and diencephalon at both 3 and 5 dpf (Figs. 2C and 2D).

Given the considerable aminergic neuron loss we identified, we next determined the specificity of DEPe-induced neurotoxicity. Nonaminergic sensory neurons expressing eGFP were quantified using the transgenic line Tg(*isl1[ss]:Gal4-VP16,UAS:eGFP*)^{zf154}, which labels both central and peripheral

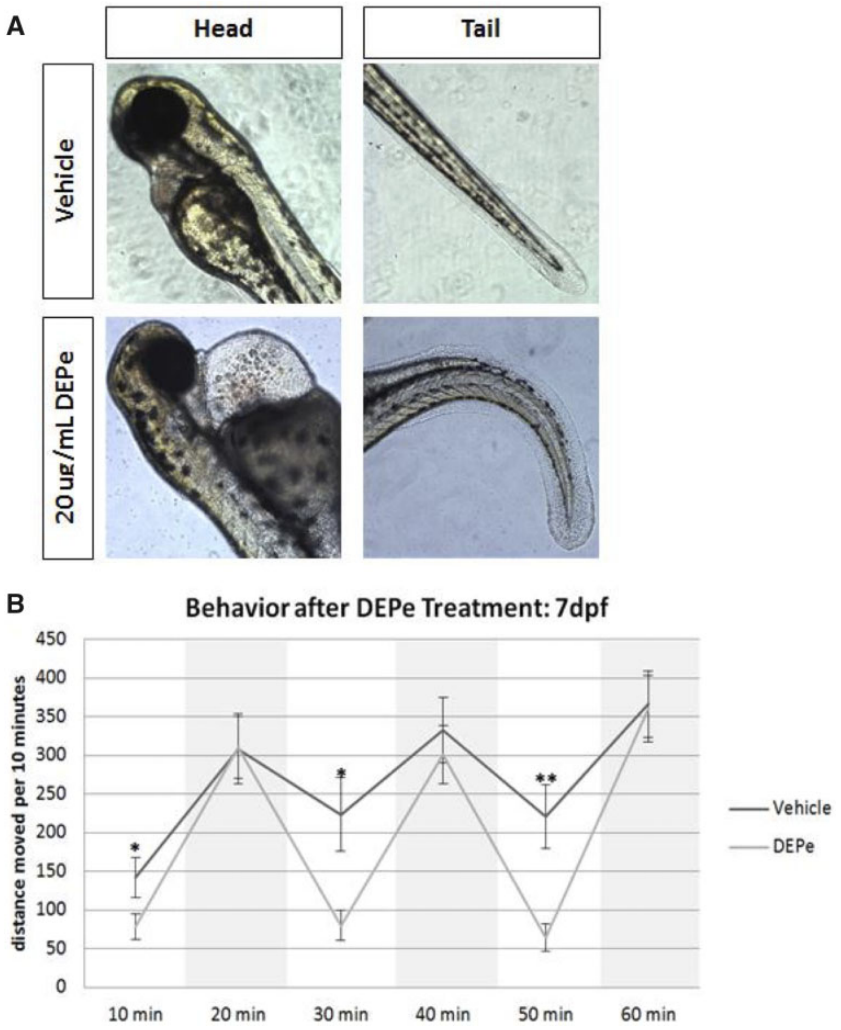

Figure 1. Diesel exhaust particulate extract toxicity in ZF. Dechorionated embryos were exposed to 20 μg/ml DEPe in 0.01% DMSO from 24 to 72 hpf and imaged for gross morphological defects in both the heart (left) as well as the tail (right) (A). Square, clear-walled 96-well plates were used for behavioral analysis in 7 dpf embryos treated with 25 μg/ml DEPe from 24 to 48 hpf and washed out. Light cycling was analyzed averaging distance moved per 10 min in both light and dark conditions (dark conditions are shaded in the graph) for 3 cycles with 9–11 larvae per condition (B). Statistical analysis by two-way ANOVA with repeated measures (*$p < .05$ and SEM).

sensory neurons and is present in early developing ZF embryos. Consistent with the loss of Vmat2+ neurons, sensory neurons in the tail region of 5 dpf larvae showed reduction in eGFP-positive neurons after DEPe treatment (Figs. 3A and 3B). Furthermore, serotonergic neurons were also reduced in the raphae nucleus at 5 dpf (Figs. 3C and 3D). Thus, a brief exposure to DEPe led to progressive and nonselective loss of neurons.

Because of the importance of alterations in protein degradation in neurodegenerative disease, we tested whether exposure to DEPe may be altering the ubiquitin proteasome system (UPS) or autophagic flux by first utilizing a sensitive and validated proteasome efficiency assay in human neuroblastoma cells (Bence *et al.*, 2001; Chou *et al.*, 2008; Wang *et al.*, 2006). In this assay, we used transformed SK-N-MC (SK-GFPu) cells, which express GFP targeted for rapid UPS degradation. Treatment with the proteasome inhibitor lactacystin showed a 2.5-fold increase in cells expressing GFP compared with control, whereas 25 μg/ml DEPe treatment showed no change in cells expressing GFP (Figure 4A), suggesting DEPe does not impact UPS activity. We next tested whether DEPe alters autophagic flux. Autophagy is dynamic and cannot be parsed by examining a single timepoint or the levels of one protein (Klionsky *et al.*, 2016). To determine the effect of DEPe on autophagic flux, we treated SK-N-MC human neuroblastoma cells for 24 h with DEPe in the presence or absence of lysosomal protease inhibitors Pepstatin A and E64D (P/E) and then measured levels of LC3II/LC3I via Western blot (Figure 4B). Treatment with P/E alone led to an increase in the ratio of LC3II/I because turnover was inhibited. After treatment with DEPe alone, the ratios of LC3II/I were unchanged. However, after DEPe treatment in combination with P/E, there was a reduction in LC3II/LC3I levels compared with P/E treatment alone, suggesting that the rate of autophagosome formation during the treatment was reduced in a manner consistent with lower autophagic turnover (Figure 4C).

To confirm the reduction in autophagic flux in vivo, we utilized a previously validated assay in transgenic ZF larvae expressing eGFP fused to Lc3 in neurons (Tg(*elavl3: eGFP: map1lc3b*)^{LA50016}) referred to as *huc*: eGFP: Lc3. Under normal conditions, eGFP: Lc3 protein is diffuse and relatively ubiquitous within neurons. Autophagosomes can be seen as small, intracellular, eGFP-positive puncta when visualized in the live animal via confocal microscopy. The number of autophagosomes

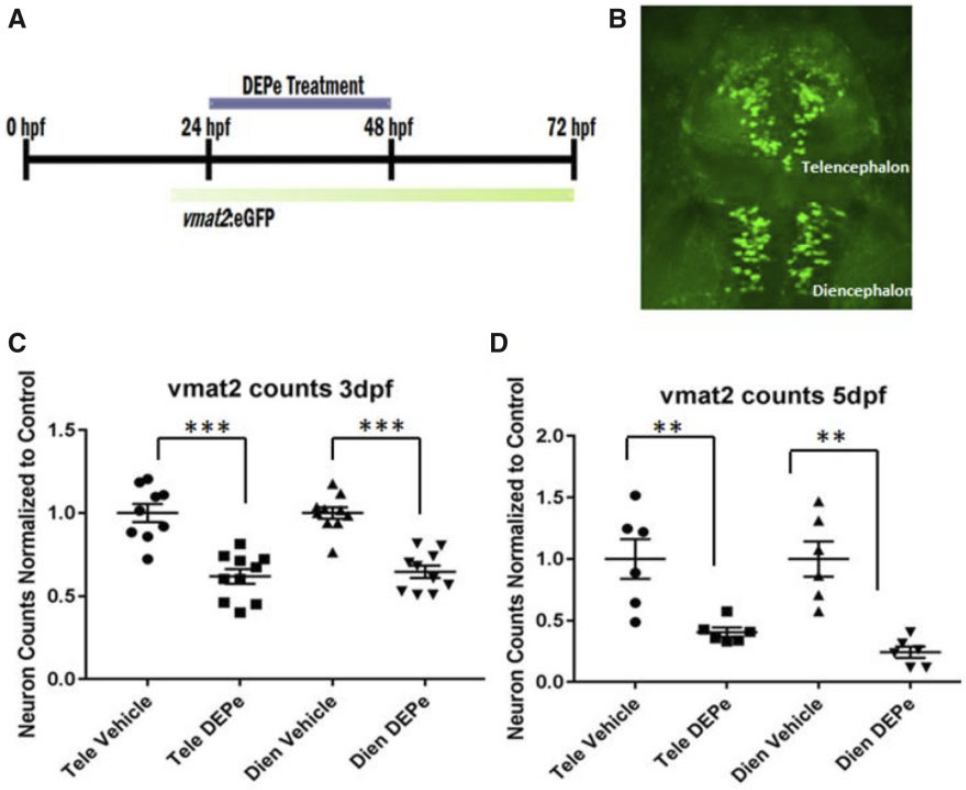

Figure 2. DEPe treatment and analysis of ZF aminergic neurons. Experimental design (A) and representative image of the aminergic neurons quantified in the *vmat2*: eGFP transgenic line (B). Vmat2+ neurons were quantified after treatment with 10 μg/ml DEPe at (C) 3 dpf or (D) 5 dpf via confocal microscopy in fixed embryos and counts were normalized to the baseline in control embryos for aminergic neurons in the telencephalon (Tele) and diencephalon (Dien). Counts from 3 and 5 dpf showed a statistically significant decrease in neurons after DEPe treatment (***$p < .0001$, **$p < .005$ as determined by one-way ANOVA with Sidak's multiple comparisons analysis and SEM).

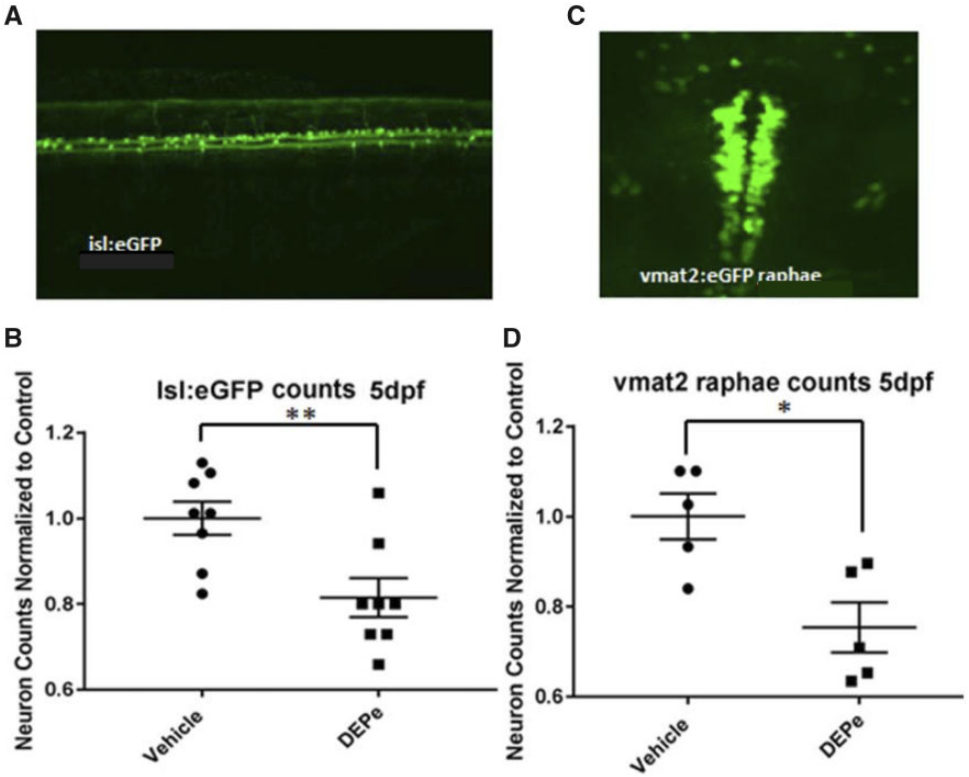

Figure 3. Specificity of neuronal toxicity after DEPe exposure. Neurons expressing GFP from the *islet1* or *vmat2* promoter were quantified at 5 dpf after 24 h of DEPe treatment in order to determine the selectivity of neurotoxicity (A). We found a significant loss of GFP-positive sensory neurons in the tail of isl:GFP embryos after treatment with 25 μg/ml DEPe (B). Statistical analysis by unpaired two-tailed Student's *t* test (**$p = .0077$) (C). Serotonergic neurons within the raphae cluster of *vmat2*: eGFP-positive embryos treated with 10 μg/ml DEPe were also significantly reduced at 3 dpf as quantified by unpaired two-tailed Student's *t* test (*$p = .011$) (D).

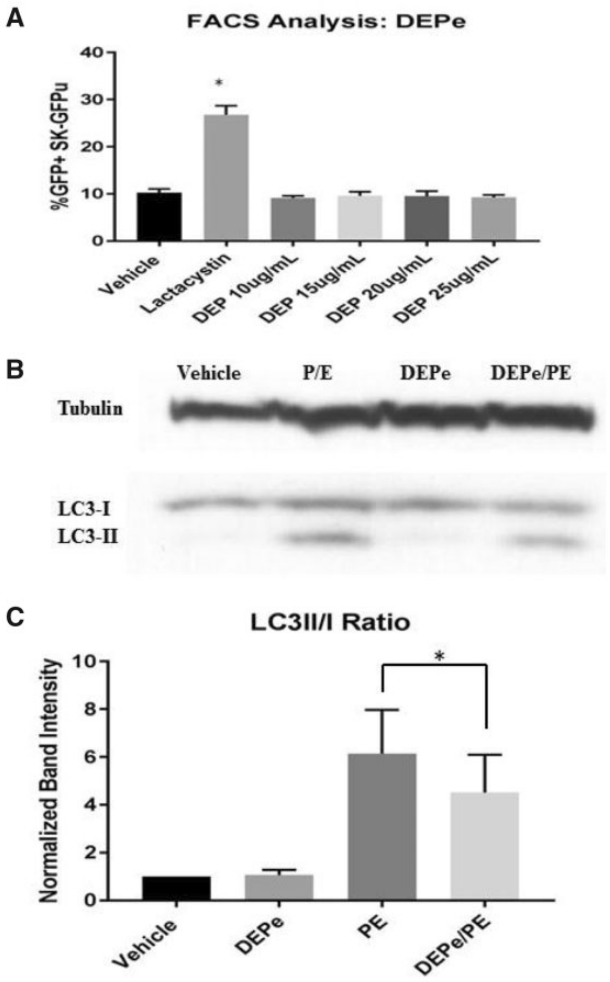

Figure 4. Proteasome function and autophagy in cells after DEPe treatment. Using SK-N-MC expressing a GFPu degron, cells were analyzed by FACS for GFP intensity after treatment with DEPe. Quantification of the % of GFP-positive cells represents the degree of proteasome inhibition. Lactacystin resulted in a statistically significant increase in GFP+ cells relative to control (2.5-fold increase), but DEPe did not alter GFP fluorescence (A). Data analysis by one-way ANOVA with Dunnett's multiple comparisons analysis (*$p = .0001$). SK-N-MC cells treated with DEPe, P/E, or both were collected for protein purification after 24 h of treatment and run on a Western blot (B). Lysosomal inhibition with P/E caused a significant increase in LC3II/I ratio, but when combined with DEPe, showed a decrease in LC3II/I, indicating lower autophagic flux (C). Quantification of $N = 5$, Western blots; *$p = .044$ by paired Student's *t* test.

is an indicator of autophagic activity, particularly when paired with inhibitors of autophagic flux as described previously (Khuansuwan *et al.*, 2019).

To determine whether DEPe acted as an inhibitor of autophagic flux in vivo, we treated *huc:* eGFP: Lc3 transgenic ZF with DEPe and lysosomal inhibitors P/E, which allowed us to quantify autophagosome turnover (Figure 5A). After treatment with DEPe for 24 h, we saw an increase in the total number of autophagosomes (Figure 5B). This could be interpreted as either an increase in autophagosome formation or a decrease in turnover. To distinguish between these two possibilities, we combined DEPe treatment with P/E. There was no difference in the total number of autophagosomes accumulated under these two conditions (Figure 5C). These findings confirm that the initial increase in autophagosome number in DEPe-treated animals was not due to increased formation, but occurred through inhibition of turnover. Thus, two independent assays measuring autophagic flux showed that DEPe reduced autophagosome turnover.

Because autophagic flux was reduced after treatment with DEPe, we measured an aggregation-prone ZF protein to determine if impaired proteostasis resulted in higher levels of toxic neuronal proteins. ZF do not have a homolog of amyloid beta or α-synuclein, but the genome does contain three synuclein family genes, including synuclein gamma 1 (Sncg1), synuclein gamma 2, and synuclein beta (Milanese *et al.*, 2012; Sun and Gitler, 2008). Based on region of expression, aggregation propensity, and neurotoxicity, Sncg1 is the closest functional paralog in the ZF embryo (Lulla *et al.*, 2016; Milanese *et al.*, 2012). To determine the impact of DEPe exposure on levels of Sncg1 in ZF larvae, they were treated with DEPe from 48 to 120 hpf and protein was analyzed for Sncg1 by Western blot. This allowed us to measure Sncg1 in the brain in the absence of neuron loss. After exposure to DEPe, the protein level of aggregated Sncg1 was significantly increased relative to control, particularly when looking at the species that corresponds to tetrameric synuclein (Figs. 5D and 5E). Unfortunately, no ZF Sncg1 antibodies exist that would allow for distinguishing between aggregated and monomeric protein. However, Sncg1 mRNA expression was reduced in the presence of DEPe (data not shown) and therefore, the protein increases cannot be accounted for by transcriptional upregulation.

Experimental results both in vivo and in vitro demonstrate that DEPe reduced autophagic activity. To test if this reduced turnover was the cause of DEPe-induced neurotoxicity, we used the drug nilotinib, which has previously been shown in ZF to increase autophagic flux (Khuansuwan *et al.*, 2019). In combination with DEPe treatment, nilotinib mitigated the DEPe-induced loss of eGFP-positive neurons in the diencephalic cluster of Vmat2+ neurons (Figs. 6A and 6B) but did not rescue morphology (data not shown). This supports the hypothesis that neurotoxicity from DEPe is caused, at least in part, by reduced autophagic activity.

DISCUSSION

In this study, we investigated the mechanisms by which exposure to diesel exhaust may alter molecular pathways that predispose individuals to neurodegenerative disease and found that DEPe exposure resulted in behavioral deficits and neurotoxicity in an in vivo vertebrate model. In two models, DEPe exposure reduced autophagic flux, which was further supported by a concurrent increase in Sncg1 protein levels in ZF larvae. Finally, using an autophagy-inducing drug treatment, we were able to rescue DEPe-induced Vmat2+ neurotoxicity.

This study expands on what is known about the mechanisms behind diesel exhaust-induced neurotoxicity and adds biological plausibility for a causal relationship to the epidemiological association between air pollution exposure and neurodegenerative disease risk. This study further underscores the importance of protein turnover as a critical pathway disrupted in neurodegenerative disease and is novel in its approach to studying environmental exposures that impact the degradation of aggregation-prone neuronal proteins in vivo. Although the change in autophagic flux in our model system appears small, it was confirmed in SK-N-MC cells and was sufficient to cause neuronal toxicity given that it was rescued using the relatively toxic drug nilotinib which we and others have shown induces autophagy (Khuansuwan *et al.*, 2019). Our ZF autophagy assay is extremely sensitive and utilizes our ability to measure neuronal autophagic flux in living intact larvae. Impaired proteostasis is

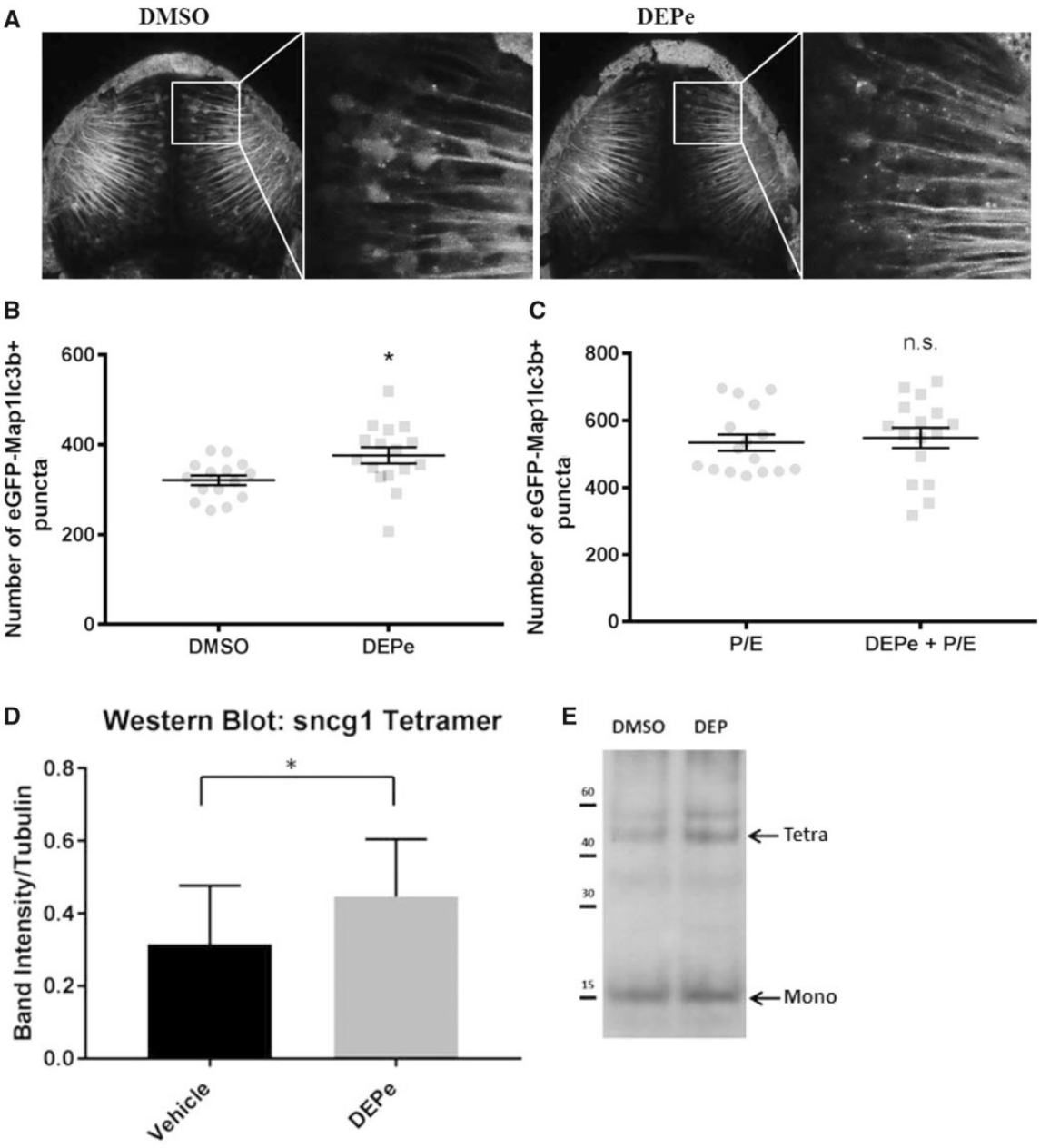

Figure 5. Effect of DEPe on autophagic turnover in ZF. Punctae quantification from confocal images of live embryos (A). There was an increase in the number of autophagosomes after DEPe treatment when compared with vehicle controls as analyzed by Student's *t* test ($p > .05$) (B). When paired with a lysosomal inhibitor, DEPe treatment did not show any additional punctae formation (C). Statistical analysis by unpaired Student's *t* test, $^*p < .05$. Western blot on protein extracted from the heads of 50 larvae per group ($N = 5$ treatments) after treatment with 10 μg/ml DEPe between 48 and 120 hpf (D). Bands were normalized to α-tubulin intensity and Sncg1 was quantified at 55 kDa, which is consistent with tetrameric synuclein. Analysis by paired Student's *t* test yielded significant differences in synuclein level ($p = .027$) (E).

further supported by the increase in Sncg1 levels although we do not believe that the accumulation of this protein is enough to account for DEPe neurotoxicity. Knocking down Sncg1 expression with morpholinos resulted in a small but not significant reduction in Vmat2+ neuron loss suggesting that impaired autophagy resulted in the accumulation of other proteins or dysfunctional organelle resulting in neuron toxicity (data not shown). Thus the elevated levels of Sncg1 is likely ran example of a protein that accumulates because of dysfunctional degradation. It is not difficult to conceive that the cumulative impact of reduced turnover of toxic proteins or organelles over years of exposure has the potential to dramatically impact the health of neurons. Interestingly, nilotinib did not rescue the morphological phenotype observed in some of the larvae, suggesting other pathways must also be impaired resulting in a more general toxicity.

These findings do not suggest that other disease-relevant pathways are not involved in air pollution-induced neurotoxicity. Indeed, it is quite clear from previous studies that neuroinflammation, among other things, is altered by exposure to diesel exhaust (Block *et al.*, 2004; Levesque *et al.*, 2011). One reason we believe this is not playing a major role in our model of toxicity is that during the time of diesel exhaust exposure, microglia are not yet active within the brain of the developing

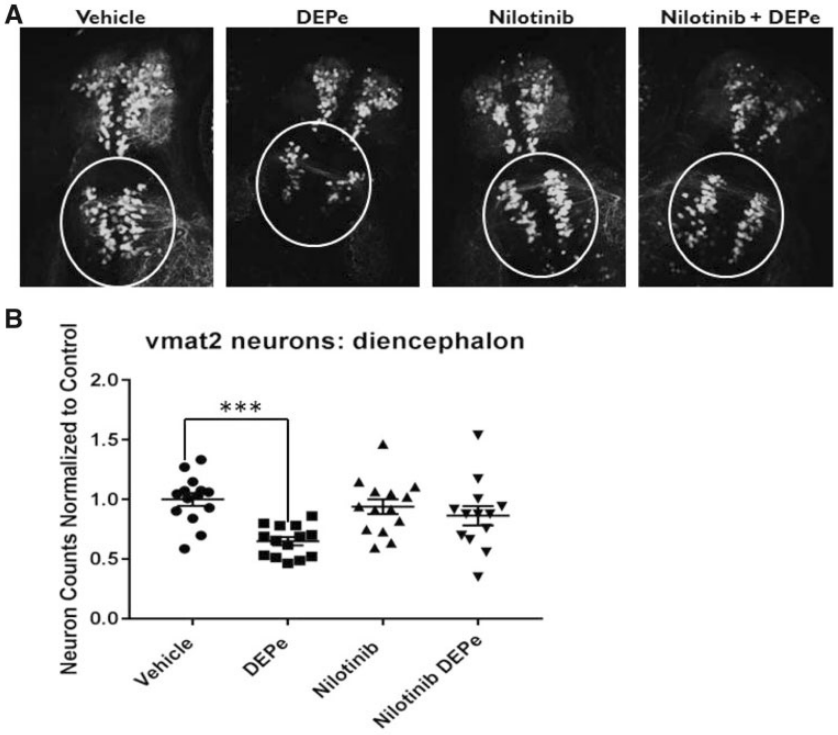

Figure 6. Testing neuroprotection with nilotinib after DEPe treatment. Vmat2 positive neuron counts from blinded confocal images after treatment with DEPe and/or nilotinib (A). Data represent diencephalic neuron counts from 3 experiments, $n = 14$ larvae normalized to control counts for each experiment. DEPe alone shows a significant reduction by one-way ANOVA with Dunnett's multiple comparison analysis (***$p = .0003$) in the number of aminergic neurons in the diencephalon (B). Neither nilotinib alone nor the combined nilotinib/DEPe treatments show a significant change in neuron number relative to control.

embryo (Rossi *et al.*, 2015). Based on previous studies, it is likely that long-term exposure to air pollution would result in neuroinflammation that could also contribute to disease risk.

One weakness of our study is that most assays were performed in developing fish larvae. This was necessary to take advantage of the fact that they are transparent at this age allowing us to assay autophagy in living intact vertebrate neurons. Because neurodegenerative disorders develop over decades, measuring the perturbation of pathways leading to the disorders has become a well-accepted approach (ie, adverse outcome pathways) (Tan *et al.*, 2018). Another potential weakness of these studies is the mode of diesel exhaust exposure; although we believe using DEPe in the water is still very relevant to human exposures. Both the olfactory and gastrointestinal systems represent major routes of environmental exposure and inhaled toxins can gain direct access to the brain via the olfactory bulb or indirectly through the bloodstream (Oberdörster *et al.*, 2004; Peiffer *et al.*, 2013; Takenaka *et al.*, 2001). It has previously been demonstrated that many components of air pollution reach the brain and can bioaccumulate (Bond *et al.*, 1986; Oberdörster *et al.*, 2004; Peiffer *et al.*, 2013; Takenaka *et al.*, 2001). Because this study utilizes diesel exhaust particulate extract, it is difficult to extrapolate to relevant human exposure levels from air pollution. However, a recent study of postmortem brain tissue found that polycyclic aromatic hydrocarbons (PAHs), thought to be some of the most biologically active components in air pollution, are not only found within the human brain but also accumulate. In this report, the mean concentration of 13 different PAHs was found to be 0.377 ng/g (Pastor-Belda *et al.*, 2019). The DEPe we utilized in our study contains 4 of these 13 PAHs including phenanthrene, pyrene, fluorene, and chrysene (Supplementary Table 1) and the average concentration of each compound that the fish were exposed to was 1.06 ng/ml. When the 13 compounds were compared directly, the mean concentration of these PAHs in our treatment was 0.32 ng/ml, which is very comparable to concentrations found within the human brain. This is particularly concerning for human health given that we are seeing dramatic toxicity at concentrations in the same range that are in our brains presumably for many years.

As pathways of critical importance are thoroughly defined, it becomes possible to begin designing disease-modifying therapeutic agents that can address the underlying mechanisms of neurotoxicity. Inducing autophagy to reduce the levels of toxic proteins in the brains of individuals with neurodegenerative disease has recently become of interest for therapeutic purposes (Martinez-Vicente and Cuervo, 2007; Menzies *et al.*, 2017; Rubinsztein *et al.*, 2012). In rodent models, treatment with the drug nilotinib has been shown to be neuroprotective and to activate the clearance of aggregated protein (Hebron *et al.*, 2013; Karuppagounder *et al.*, 2015; Lonskaya *et al.*, 2014). Although still in preliminary stages of investigation, this class of drugs has shown promise in several model systems and lends credence to the idea that impaired autophagy is a primary molecular mechanism of neurotoxicity in neurodegenerative disease.

SUPPLEMENTARY DATA

Supplementary data are available at *Toxicological Sciences* online.

ACKNOWLEDGMENT

The authors especially thank Alvaro Sagasti for the use of the transgenic ZF line Tg(*isl1[ss]:Gal4-VP16,UAS:eGFP*)^{zf154}.

FUNDING

National Institute of Environmental Health Sciences, National Institutes of Health, RO1 Award ES016959 (to J.A.A.), NIEHS T32ES015457 (to L.M.B., S.K.), the Levine Foundation, and the Parkinson's Alliance.

AUTHOR CONTRIBUTIONS

L.M.B. and S.K. designed experiments. L.M.B., S.K., and H.M. acquired data and interpreted results. D.J. acquired and analyzed data. J.M.B. and J.A.A. contributed to the design of the study and the analysis of data. J.M.B. and L.M.B. contributed to the drafting and revision of the manuscript.

DECLARATION OF CONFLICTING INTERESTS

The authors declared no potential conflicts of interest with respect to the research, authorship, and/or publication of this article.

References

Bandmann, O., and Burton, E. A. (2010). Genetic zebrafish models of neurodegenerative diseases. *Neurobiol. Dis.* **40**, 58–65.

Bence, N. F., Sampat, R. M., and Kopito, R. R. (2001). Impairment of the ubiquitin-proteasome system by protein aggregation. *Science* **292**, 1552–1555.

Betarbet, R., Canet-Aviles, R. M., Sherer, T. B., Mastroberardino, P. G., McLendon, C., Kim, J.-H., Lund, S., Na, H.-M., Taylor, G., Bence, N. F., *et al.* (2006). Intersecting pathways to neurodegeneration in Parkinson's disease: Effects of the pesticide rotenone on DJ-1, alpha-synuclein, and the ubiquitin-proteasome system. *Neurobiol. Dis.* **22**, 404–420.

Block, M. L., Wu, X., Pei, Z., Li, G., Wang, T., Qin, L., Wilson, B., Yang, J., Hong, J. S., Veronesi, B., *et al.* (2004). Nanometer size diesel exhaust particles are selectively toxic to dopaminergic neurons: The role of microglia, phagocytosis, and NADPH oxidase. *FASEB J.* **18**, 1618–1620.

Bond, J. A., Ayres, P. H., Medinsky, M. A., Cheng, Y. S., Hirshfield, D., and McClellan, R. O. (1986). Disposition and metabolism of [14C]dibenzo[c, g]carbazole aerosols in rats after inhalation. *Fundam. Appl. Toxicol.* **7**, 76–85.

Calderón-Garcidueñas, L., Kavanaugh, M., Block, M., D'Angiulli, A., Delgado-Chávez, R., Torres-Jardón, R., González-Maciel, A., Reynoso-Robles, R., Osnaya, N., Villarreal-Calderon, R., *et al.* (2012). Neuroinflammation, hyperphosphorylated tau, diffuse amyloid plaques, and down-regulation of the cellular prion protein in air pollution exposed children and young adults. *J. Alzheimers Dis.* **28**, 93–107.

Calderón-Garcidueñas, L., Mora-Tiscareño, A., Ontiveros, E., Gómez-Garza, G., Barragán-Mejía, G., Broadway, J., Chapman, S., Valencia-Salazar, G., Jewells, V., Maronpot, R. R., *et al.* (2008). Air pollution, cognitive deficits and brain abnormalities: A pilot study with children and dogs. *Brain Cogn.* **68**, 117–127.

Chou, A. P., Maidment, N., Klintenberg, R., Casida, J. E., Li, S., Fitzmaurice, A. G., Fernagut, P.-O., Mortazavi, F., Chesselet, M.-F., Bronstein, J. M., *et al.* (2008). Ziram causes dopaminergic cell damage by inhibiting E1 ligase of the proteasome. *J. Biol. Chem.* **283**, 34696–34703.

Costa, L. G., Cole, T. B., Coburn, J., Chang, Y. C., Dao, K., and Roque, P. (2014). Neurotoxicants are in the air: Convergence of human, animal, and in vitro studies on the effects of air pollution on the brain. *BioMed Res. Int.* **2014**, 1–8.

Dimakakou, E., Johnston, H. J., Streftaris, G., and Cherrie, J. W. (2018). Exposure to environmental and occupational particulate air pollution as a potential contributor to neurodegeneration and diabetes: A systematic review of epidemiological research. *Int. J. Environ. Res. Public Health* **15**, 1–37.

Elbaz, A., Dufouil, C., and Alperovitch, A. (2007). Interaction between genes and environment in neurodegenerative diseases. *Compt. Rend. Biol.* **330**, 318–328.

Fu, P., Guo, X., Cheung, F. M. H., and Yung, K. (2019). The association between PM2.5 exposure and neurological disorders: A systematic review and meta-analysis. *Sci. Total Environ.* **655**, 1240–1248.

Ghiglieri, V., Calabrese, V., and Calabresi, P. (2018). Alpha-synuclein: From early synaptic dysfunction to neurodegeneration. *Front. Neurol.* **9**, 295.

Goldman, S. M., Kamel, F., Ross, G. W., Jewell, S. A., Bhudhikanok, G. S., Umbach, D., Marras, C., Hauser, R. A., Jankovic, J., Factor, S. A., *et al.* (2012). Head injury, alpha-synuclein Rep1, and Parkinson's disease. *Ann. Neurol.* **71**, 40–48.

Guarnieri, M., and Balmes, J. R. (2014). Outdoor air pollution and asthma. *Lancet* **383**, 1581–1592.

Hebron, M. L., Lonskaya, I., and Moussa, C. E. (2013). Nilotinib reverses loss of dopamine neurons and improves motor behavior via autophagic degradation of alpha-synuclein in Parkinson's disease models. *Hum. Mol. Genet.* **22**, 3315–3328.

Hesterberg, T. W., Long, C. M., Lapin, C. A., Hamade, A. K., and Valberg, P. A. (2010). Diesel exhaust particulate (DEP) and nanoparticle exposures: What do DEP human clinical studies tell us about potential human health hazards of nanoparticles? *Inhal Toxicol.* **22**, 679–694.

Heusinkveld, H. J., Wahle, T., Campbell, A., Westerink, R. H. S., Tran, L., Johnston, H., Stone, V., Cassee, F. R., and Schins, R. P. F. (2016). Neurodegenerative and neurological disorders by small inhaled particles. *Neurotoxicology* **56**, 94–106.

Hoek, G., Brunekreef, B., Fischer, P., and van Wijnen, J. (2001). The association between air pollution and heart failure, arrhythmia, embolism, thrombosis, and other cardiovascular causes of death in a time series study. *Epidemiology* **12**, 355–357.

Hu, C.-Y., Fang, Y., Li, F.-L., Dong, B., Hua, X.-G., Jiang, W., Zhang, H., Lyu, Y., and Zhang, X.-J. (2019). Association between ambient air pollution and Parkinson's disease: Systematic review and meta-analysis. *Environ. Res.* **168**, 448–459.

Jellinger, K. A. (2010). Basic mechanisms of neurodegeneration: A critical update. *J. Cell. Mol. Med.* **14**, 457–487.

Karuppagounder, S. S., Brahmachari, S., Lee, Y., Dawson, V. L., Dawson, T. M., and Ko, H. S. (2015). The c-Abl inhibitor, nilotinib, protects dopaminergic neurons in a preclinical animal model of Parkinson's disease. *Sci. Rep.* **4**, 4874.

Khuansuwan, S., Barnhill, L. M., Cheng, S., and Bronstein, J. M. (2019). A novel transgenic zebrafish line allows for in vivo quantification of autophagic activity in neurons. *Autophagy* **15**, 1322–1311.

Klionsky, D. J., Abdelmohsen, K., Abe, A., Abedin, M. J., Abeliovich, H., Acevedo Arozena, A., Adachi, H., Adams, C. M., Adams, P. D., Adeli, K., *et al.* (2016). Guidelines for the use and interpretation of assays for monitoring autophagy (3rd edition). *Autophagy* **12**, 1–222.

Lawal, A., Zhang, M., Dittmar, M., Lulla, A., and Araujo, J. A. (2015). Heme oxygenase-1 protects endothelial cells from the toxicity of air pollutant chemicals. *Toxicol. Appl. Pharmacol.* **284**, 281–291.

Lee, K. K., Miller, M. R., and Shah, A. (2018). Air Pollution and Stroke. *J. Stroke* **20**, 2–11.

Lee, P. C., Bordelon, Y., Bronstein, J., Sinsheimer, J. S., Farrer, M., and Ritz, B. (2015). Head injury, alpha-synuclein genetic variability and Parkinson's disease. *Eur. J. Neurol.* **22**, 874–878.

Levesque, S., Surace, M. J., McDonald, J., and Block, M. L. (2011). Air pollution & the brain: Subchronic diesel exhaust exposure causes neuroinflammation and elevates early markers of neurodegenerative disease. *J. Neuroinflam.* **8**, 105.

Levesque, S., Taetzsch, T., Lull, M. E., Kodavanti, U., Stadler, K., Wagner, A., Johnson, J. A., Duke, L., Kodavanti, P., Surace, M. J., *et al.* (2011). Diesel exhaust activates and primes microglia: Air pollution, neuroinflammation, and regulation of dopaminergic neurotoxicity. *Environ. Health Perspect.* **119**, 1149–1155.

Lonskaya, I., Hebron, M. L., Desforges, N. M., Schachter, J. B., and Moussa, C. E. (2014). Nilotinib-induced autophagic changes increase endogenous parkin level and ubiquitination, leading to amyloid clearance. *J. Mol. Med.* **92**, 373–386.

Lulla, A., Barnhill, L., Bitan, G., Ivanova, M. I., Nguyen, B., O'Donnell, K., Stahl, M. C., Yamashiro, C., Klärner, F.-G., Schrader, T., *et al.* (2016). Neurotoxicity of the Parkinson disease-associated pesticide ziram is synuclein-dependent in zebrafish embryos. *Environ. Health Perspect.* **124**, 1766–1775.

Martin-Jimenez, R., Campanella, M., and Russell, C. (2015). New zebrafish models of neurodegeneration. *Curr. Neurol. Neurosci. Rep.* **15**, 33.

Martinez-Vicente, M., and Cuervo, A. M. (2007). Autophagy and neurodegeneration: When the cleaning crew goes on strike. *Lancet Neurol.* **6**, 352–361.

Menzies, F. M., Fleming, A., Caricasole, A., Bento, C. F., Andrews, S. P., Ashkenazi, A., Füllgrabe, J., Jackson, A., Jimenez Sanchez, M., Karabiyik, C., *et al.* (2017). Autophagy and neurodegeneration: Pathogenic mechanisms and therapeutic opportunities. *Neuron* **93**, 1015–1034.

Milanese, C., Sager, J. J., Bai, Q., Farrell, T. C., Cannon, J. R., Greenamyre, J. T., and Burton, E. A. (2012). Hypokinesia and reduced dopamine levels in zebrafish lacking beta- and gamma1-synucleins. *J. Biol. Chem.* **287**, 2971–2983.

Mustafić, H., Jabre, P., Caussin, C., Murad, M. H., Escolano, S., Tafflet, M., Périer, M.-C., Marijon, E., Vernerey, D., Empana, J.-P., *et al.* (2012). Main air pollutants and myocardial infarction: A systematic review and meta-analysis. *JAMA* **307**, 713–721.

Oberdörster, G., Sharp, Z., Atudorei, V., Elder, A., Gelein, R., Kreyling, W., and Cox, C. (2004). Translocation of inhaled ultrafine particles to the brain. *Inhal. Toxicol.* **16**, 437–445.

Ohama, E., and Ikuta, F. (1976). Parkinson's disease: Distribution of Lewy bodies and monoamine neuron system. *Acta Neuropathol.* **34**, 311–319.

Palacios, N. (2017). Air pollution and Parkinson's disease - Evidence and future directions. *Rev. Environ. Health* **32**, 303–313.

Palanca, A. M. S., Lee, S.-L., Yee, L. E., Joe-Wong, C., Trinh, L. A., Hiroyasu, E., Husain, M., Fraser, S. E., Pellegrini, M., Sagasti, A., *et al.* (2013). New transgenic reporters identify somatosensory neuron subtypes in larval zebrafish. *Dev. Neurobiol.* **73**, 152–167.

Pastor-Belda, M., Campillo, N., Arroyo-Manzanares, N., Torres, C., Pérez-Cárceles, M. D., Hernández-Córdoba, M., and Viñas, P. (2019). Bioaccumulation of polycyclic aromatic hydrocarbons for forensic assessment using gas chromatography-mass spectrometry. *Chem. Res. Toxicol.* **32**, 1680–1688.

Peiffer, J., Cosnier, F., Grova, N., Nunge, H., Salquèbre, G., Decret, M.-J., Cossec, B., Rychen, G., Appenzeller, B. M. R., Schroeder, H., *et al.* (2013). Neurobehavioral toxicity of a repeated exposure (14 days) to the airborne polycyclic aromatic hydrocarbon fluorene in adult Wistar male rats. *PLoS One* **8**, e71413.

Ritz, B., Lee, P.-C., Hansen, J., Lassen, C. F., Ketzel, M., Sørensen, M., and Raaschou-Nielsen, O. (2016). Traffic-related air pollution and Parkinson's disease in Denmark: A case-control study. *Environ. Health Perspect.* **124**, 351–356.

Ross, C. A., and Poirier, M. A. (2004). Protein aggregation and neurodegenerative disease. *Nat. Med.* **10**, S10–S17.

Rossi, F., Casano, A. M., Henke, K., Richter, K., and Peri, F. (2015). The SLC7A7 transporter identifies microglial precursors prior to entry into the brain. *Cell Rep.* **11**, 1008–1017.

Rubinsztein, D. C., Codogno, P., and Levine, B. (2012). Autophagy modulation as a potential therapeutic target for diverse diseases. *Nat. Rev. Drug Discov.* **11**, 709–730.

Shou, Y., Huang, Y., Zhu, X., Liu, C., Hu, Y., and Wang, H. (2019). A review of the possible associations between ambient PM2.5 exposures and the development of Alzheimer's disease. *Ecotoxicol. Environ. Saf.* **174**, 344–352.

Spillantini, M. G., Schmidt, M. L., Lee, V. M., Trojanowski, J. Q., Jakes, R., and Goedert, M. (1997). Alpha-synuclein in Lewy bodies. *Nature* **388**, 839–840.

Sun, Z., and Gitler, A. D. (2008). Discovery and characterization of three novel synuclein genes in zebrafish. *Dev. Dyn.* **237**, 2490–2495.

Suzuki, T., Oshio, S., Iwata, M., Saburi, H., Odagiri, T., Udagawa, T., Sugawara, I., Umezawa, M., and Takeda, K. (2010). In utero exposure to a low concentration of diesel exhaust affects spontaneous locomotor activity and monoaminergic system in male mice. *Part. Fibre Toxicol.* **7**, 7.

Takenaka, S., Karg, E., Roth, C., Schulz, H., Ziesenis, A., Heinzmann, U., Schramel, P., and Heyder, J. (2001). Pulmonary and systemic distribution of inhaled ultrafine silver particles in rats. *Environ. Health Perspect.* **109(Suppl. 4)**, 547–551.

Tan, Y. M., Leonard, J. A., Edwards, S., Teeguarden, J., Paini, A., and Egeghy, P. (2018). Aggregate exposure pathways in support of risk assessment. *Curr. Opin. Toxicol.* **9**, 8–13.

Taylor, J. P., Hardy, J., and Fischbeck, K. H. (2002). Toxic proteins in neurodegenerative disease. *Science* **296**, 1991–1995.

Vegh, C., Stokes, K., Ma, D., Wear, D., Cohen, J., Ray, S. D., and Pandey, S. (2019). A bird's-eye view of the multiple biochemical mechanisms that propel pathology of Alzheimer's disease: recent advances and mechanistic perspectives on how to halt the disease progression targeting multiple pathways. *J. Alzheimers Dis.* **69**, 631–649.

Wang, X. F., Li, S., Chou, A. P., and Bronstein, J. M. (2006). Inhibitory effects of pesticides on proteasome activity: Implication in Parkinson's disease. *Neurobiol. Dis.* **23**, 198–205.

Wen, L., Wei, W., Gu, W., Huang, P., Ren, X., Zhang, Z., Zhu, Z., Lin, S., and Zhang, B. (2008). Visualization of monoaminergic neurons and neurotoxicity of MPTP in live transgenic zebrafish. *Dev. Biol.* **314**, 84–92.

Yokota, S., Moriya, N., Iwata, M., Umezawa, M., Oshio, S., and Takeda, K. (2013). Exposure to diesel exhaust during fetal period affects behavior and neurotransmitters in male offspring mice. *J. Toxicol. Sci.* **38**, 13–23.